

The Mechanism of Extraction of Peanut Protein and Oil Bodies by Enzymatic Hydrolysis of the Cell Wall

Chen Liu¹, Li-hua Hao², Fusheng Chen³, and Ting-wei Zhu³

¹Affiliation not available

²Henan Institute of Product Quality Supervision and Inspection

³Henan University of Technology

April 28, 2020

Abstract

Degradation of the peanut cell wall is a critical step in the aqueous enzymatic extraction process to extract proteins and oil bodies. Viscozyme® L, a compound cell wall degrading enzyme, has been applied as an alternative to protease in the process of aqueous enzymatic extraction, but the mechanism of cell wall enzymolysis remains unclear. The present study aims to investigate the changes in cellulose, hemicellulose, and pectin content of the peanut cell wall hydrolyzed by Viscozyme® L. The degree to which the main components of the peanut cell wall, such as trans-1, 2-cyclohexanediamine-N,N',N'-acetic acid-soluble pectin (CDTA-soluble pectin), Na₂CO₃-soluble pectin, cellulose, and hemicellulose, are degraded is closely related to the extraction of oil bodies and peanut protein at different solid-liquid ratio of powered peanut seed in distilled water, enzyme concentration, enzyme hydrolysis temperature, and enzyme hydrolysis time. The key sites of Viscozyme® L activity on cell wall polysaccharides were explored by comparing the changes in chemical bonds under different extraction conditions using Fourier-transform infrared spectroscopy (FT-IR) absorption bands and principal component analysis (PCA). Viscozyme® L acted on the C-O stretching, C-C stretching, and CH₂ symmetrical bending of cellulose, the C-O stretching and O-C-O asymmetrical bending of hemicellulose, and the C-O stretching and C-C stretching of pectin.

1. Introduction

Aqueous enzymatic extraction is a promising method for extraction of oils and proteins from oilseeds, in which water is used as the extraction solvent (Liu, Gasmalla, & Li, 2016). Compared with the traditional oil extraction process, aqueous enzymatic extraction has the advantages of being environmentally friendly, nonuse of organic solvents, low energy consumption, and mild reaction conditions (Li, Qi, & Sui, 2016; Yusoff, Gordon, & Niranjana, 2015). Furthermore, peanut oil requires low degree of refinement and peanut protein can be recycled at the same time (Campbell & Glatz, 2011; Latif, Anwar, & Hussain, 2011; Balvardi, Rezaei, & Mendiola, 2015). Cell wall degrading enzymes, such as cellulase, hemicellulase, and pectinase, can degrade the main components and destroy the structure of the cell wall without affecting the peanut protein. Bisht et al. (2015) showed that cellulase, hemicellulase, and pectinase alone or their complex enzymes could effectively increase the oil yield at appropriate concentrations; e.g., the combination of cellulase and pectinase increased the oil yield by 14.22%. Szydłowska-Czerniak et al. (2010) reported a higher yield of rapeseed oil extracted by pectinase and cellulase compared with the yield obtained by traditional methods, with pectinase having better effect on extracting rapeseed oil than cellulase. The degradation of the peanut cell wall in aqueous enzymatic extraction is a critical step that facilitates the release of peanut proteins and oil bodies. Viscozyme® L, a compound cell wall degradation enzyme, promotes the release of nonhydrolyzed protein and oil bodies by degrading the main components and destroy the structure of the cell wall without affecting the peanut protein (Zúñiga, Soto, & Mora, 2003; Gaur, Sharma, & Khare, 2007), but enzyme active sites of

Viscozyme[®] L and the mechanism of degradation of the peanut cell wall in aqueous enzymatic extraction remain unclear.

Fourier-transform infrared spectroscopy (FT-IR) has been applied to monitor the extraction of cell wall polysaccharides and to observe the changes in the cell wall during the processing and quality control of fruits and vegetables (Barros, Mafra, & Ferreira, 2002; Ferreira, Barros, & Coimbra, 2001). The optimal region of FT-IR spectrum used for carbohydrate analysis is 1200 - 850 cm⁻¹ and 1800 - 1200 cm⁻¹; the former region is not affected by the spectrum bands of proteins and water molecules (Coimbra, Barros, & Barros, 1998). The region 1200 - 850 cm⁻¹ mainly reflects the stretching and vibration characteristics of C-O, C-C, and CH₂ groups or the ring structure formed by these groups (Fry, 1988). To obtain relatively complete cell wall information, both regions, 1800–1200cm⁻¹ and 1200–850cm⁻¹, were used for FT-IR spectrum analysis in this study. Principal component analysis (PCA) is a common data statistics method used to simplify and analyze highly dimensional data sets by constructing principle components (PCs) that explain the maximum variability of the data. PCA is particularly suitable for analysis of the infrared spectrum characteristics in relation to sample diversity and complexity (He, 2015). FT-IR spectroscopy combined with PCA is very useful for determining structural and compositional changes in the cell wall (Ferreira, Barros, & Coimbra, 2001; Ana, Encina, & Penélope, 2004), for assessing the degree of amidation and methyl esterification of pectic polysaccharides in plant cell wall extracts (Gnanasambandam & Proctor, 2000; Winning, Viereck, & Salomonsen, 2009), and for evaluating cell wall polysaccharides composition of pectic and hemicellulosic components derived from plant materials (Hori & Sugiyama, 2003).

In the present study, the changes in cellulose, hemicellulose, and pectin content in the peanut cell wall hydrolyzed by Viscozyme[®] L were examined under different solid-liquid ratios, enzyme concentrations, enzyme hydrolysis temperatures, and enzyme hydrolysis times. The characteristic FT-IR absorption bands of cellulose, hemicellulose, and pectin in the cell wall of peanut were analyzed by PCA to explore the key sites of Viscozyme[®] L activity on peanut cell wall during enzymatic hydrolysis. The mechanism of cell wall enzymolysis studied in this paper will provide theoretical basis for further explorations of the mechanism of aqueous enzymatic extraction and help to enhance the extraction of peanut protein and oil bodies.

2. Materials and Methods

2.1. Materials

Peanut seeds were purchased from the local market (Zhengzhou, China) and stored at 4 °C until their use. The seeds were composed of (g/100 g dry matter) 46.84% oil, 24.44% protein, 4.65% crude fiber, 4.63% water, and 2.35% ash. Viscozyme[®] L (complex plant hydrolase; 5086 U/mL; the main ingredients are cellulase, hemicellulose, and arabinose) was purchased from Novozymes (Novo, China). All other reagents used were of analytical grade.

2.2. Extraction of proteins and oil bodies

Peanut protein and oil bodies were extracted using the graded extraction method (Sukhotu, 2014) and aqueous enzymatic extraction of maize germ (Li, Peng, & Li, 2015), respectively, with some modifications. The skinless peanut seeds were ground in a high-speed universal grinder (FW-100; Beijing Ever Bright Medical Treatment Inc, Beijing, China). Twenty grams of peanut powder was dispersed in deionized water (the solid-to-liquid ratio of 1:7, 1:6, 1:5, 1:4, 1:3, and 1:2 w/v). Viscozyme[®] L (0.25, 0.50, 0.75, 1.00, 1.25, 1.50, 1.75, and 2.0%, calculated by the weight of total substrate) was added to the mixture and enzymolysis was conducted in a digital water-bathing constant temperature vibrator (THZ-82; Jinhua Huafeng Instrument Inc, Jinhua, China) for different times (20, 40, 60, 80, 100, 120, and 140 min) and at different temperatures (35, 40, 45, 50, 55, 60, 65, and 70 °C). Thereafter, the enzyme was deactivated by placing the samples in a boiling water bath for 5 min. The cooled solution was centrifuged at 5000 × *g* for 20 min (DZ267-32C6; Anting Scientific Instrument Factory, Shanghai, China). The supernatant (oil bodies) was decanted and dried at 50 °C for 10 h in a vacuum drying oven (DZF-2B; Beijing Ever Bright Medical Treatment Inc, Beijing, China), whereas the precipitation was dried in a freezer dryer (LGJ-25; Beijing Sihuan Scientific Instrument Inc, Beijing, China) for 24 h and weighed. The amount of protein was measured by an Automatic Kjeldahl

Apparatus (K1100; Jinan Haineng Instrument Inc, Shandong, China), and the yields of protein and oil bodies were calculated using the formula 1 and 2, respectively:

$$\text{Yield of peanut protein} = \frac{\text{protein content of precipitate}}{\text{protein content of peanut}} \times 100 \quad (\%) \quad (1)$$

$$\text{Yield of oil bodies} = \frac{\text{dry weight of oil bodies}}{\text{weight of peanut sample}} \times 100 \quad (\%) \quad (2)$$

2.3. Extraction and determination of the main cell wall components

Sodium dodecyl sulfate solution (15 g/L, containing 5 mmol/L pyrosulfite) was added to the dried precipitate obtained as described in 2.2 and centrifuged twice at $4000 \times g$ for 15 min. The new precipitate was treated with 90% dimethyl sulfoxide to remove starch and then cleaned by several cycles of washing with distilled water and centrifugation to obtain cell wall material (CWM) (Li, Han, & Jin, 2014). The CWM was treated with 50 mL 2-cyclohexanedi-amine-*N,N,N',N'*-acetic acid (CDTA; 50 mmol/L, pH 6.5) for 6 h at 25 °C. CDTA-soluble pectin in the supernatant was obtained by filtration through a nylon membrane with 10 μm pore diameter. The remaining solid was incubated in 50 mL Na_2CO_3 solution (50 mmol/L, containing 20 mmol/L NaBH_4) at 25 °C for 6 h. Na_2CO_3 -soluble pectin in the supernatant was obtained by filtration through a nylon membrane with 10 μm pore diameter. Cellulose in the supernatant and hemicellulose in the precipitation were obtained after adding 50 mL 4 M potassium hydroxide to the remaining solid and reacting for 12 h at 25 °C (He, 2015). The amount of pectin was determined by the carbazole colorimetric method (Hou, 2004), and the amount of hemicellulose and cellulose was determined by the anthrone colorimetric method (Han, 1992; Gao, 2006).

2.4. Analysis of cell wall components by FT-IR

The infrared spectra of the peanut cell wall were assembled from 64 scans obtained at a resolution of 4 cm^{-1} between 4000 and 650 cm^{-1} using a Fourier-transform spectrometer VERTEX 70 (Bruker, Ettlingen, Germany) (Szymanska-Chargot & Zdunek, 2013).

2.5. Statistical analysis

All the experiments were carried out at least three times using duplicate samples, and the results are presented as mean \pm standard deviation. The data were statistically analyzed using Design Expert 8.05b, Origin 8.5, and SPSS 19.0. A value of $P < 0.05$ was considered statistically significant.

3. Results and Discussion

3.1. Effects of enzyme hydrolysis parameters on the yield of protein and oil bodies

The extraction rate of protein reached maximum value (88.69%) at 1:2 solid- liquid ratio, but decreased and tended to level out as the ratio increased (Fig. 1a). Such a trend could be attributed to gradual dissolution of water-soluble whey protein and salt-soluble arachin and conarachin with the increase in the solid-to-liquid ratio until reaching the threshold at which arachin and conarachin were non-degradable due to their stable spatial structure (XU, LIU, & SHI, 2016; LIU, ZHAO, & SU, 2013). The yield of oil bodies increased and then decreased; it reached the maximum (42.37%) at the solid- liquid ratio of 1:4. The increase in the aqueous solution promoted the decomposition of peanut cell wall structure, but further increase in the solid-liquid ratio reduced the enzyme activity, resulting in decreased yield of oil bodies. The yield of both protein and oil bodies initially increased and then decreased, with both reaching maximum levels (68.45% and 39.28%, respectively) at the enzyme concentration of 1.25% (Fig. 1b). Increasing the enzyme concentration to a certain level increased the degree of cell wall damage and allowed that protein and oil bodies were released in the cell at a relatively stable rate. The efficiency of enzyme hydrolysis is highly dependent on temperature. The effect of different enzyme hydrolysis temperature on the yield of protein and oil bodies is shown in Fig. 1c. The protein yield decreased after an initial increase, reaching maximum levels (78.86%) at 55 °C. The yield of oil bodies followed the same trend, but reached the maximum (38.86%) at 50 °C. The protein yield

reached maximum levels (79.91%) at 80 min, whereas the yield of oil bodies started increasing at 20 min and plateaued at 80 min (Fig. 1d). The rate of enzymatic hydrolysis was increased fast initially as the enzyme bound with the substrate. However, as the reaction progressed, the concentration of the substrate and the reaction rate decreased, and the yield of protein oil bodies stabilized.

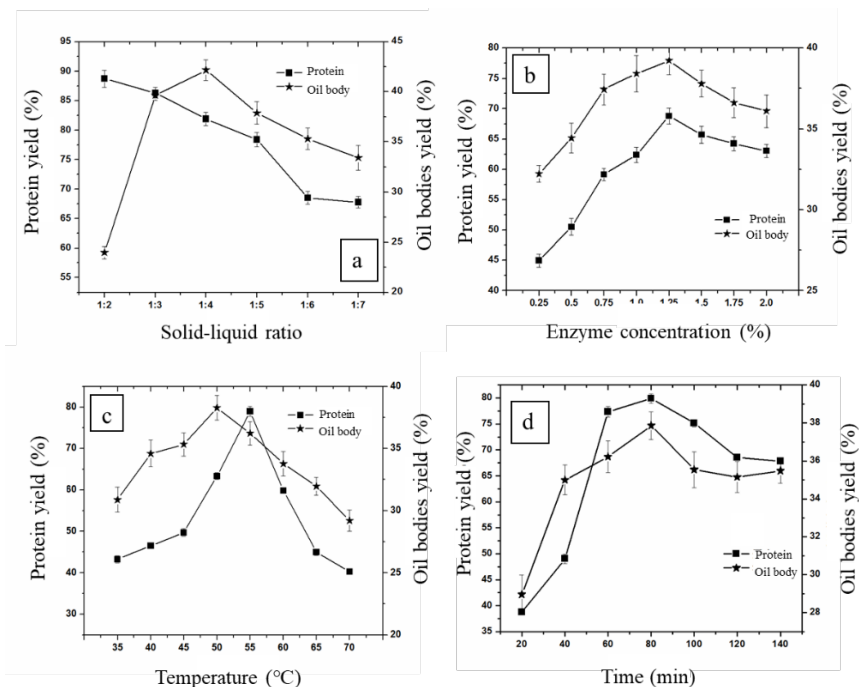


Fig. 1 Effect of enzyme hydrolysis temperature, solid-liquid ratio, enzyme concentration, and enzyme hydrolysis time on the yield of peanut protein and oil bodies.

Cell wall, which consists of cellulose, hemicellulose, and pectin, blocks the release of proteins and oil bodies outside the cell and the penetration of external solvents into the cell. Thus, the degradation of the cell wall is an important step in the extraction of protein and oil bodies. The above results indicate a close correlation of the yield of both protein and oil bodies with the operational parameters, but how the degradation of main components in the peanut cell wall affected the yield of protein and oil bodies was unclear. To address this question, we investigated the effect of Viscozyme[®] L on the main compounds of the peanut cell wall.

3.2. Degradation of the main components in peanut cell wall

Viscozyme[®] L, as a complex plant hydrolase, decomposes the cell wall structure. During the process of aqueous enzymatic extraction, the main components in the wall, cellulose, hemicellulose and pectin, are progressively degraded, meanwhile protein and oil bodies are gradually released. To elucidate the degradation of the cell wall in the aqueous enzymatic extraction process in more detail, we analyzed the changes in the main cell wall components (Table 1).

The maximum degradation rate of CDTA-soluble pectin (67.4%), Na₂CO₃-soluble pectin (87.0%), hemicellulose (39.1%), and cellulose (57.1%) was reached at solid-liquid ratios of 1:3, 1:4, 1:5, and 1:3, respectively (Table 1). A high protein yield (86.64%) and the maximum yield of oil bodies (42.18%) were recorded at solid-liquid ratios of 1:3 and 1:4, at which the degradation rates of CDTA-soluble pectin, Na₂CO₃-soluble pectin, and cellulose were the highest (Fig. 1, Table 1). The highest degradation rate of CDTA-soluble pectin (81.1%), Na₂CO₃-soluble pectin (76.0%), hemicellulose (62.7%), and cellulose (55.1%) were obtained at enzyme concentrations of 1.00, 1.25, 0.75, and 1.00%, respectively. The highest protein yield (77.86%)

and the maximum yield of oil bodies (35.76%) was attained at enzyme concentration of 1.25%, at which Na_2CO_3 -soluble pectin had the best degradation rate (Fig. 1, Table 1). Enzyme hydrolysis parameters had a significant effect on the content of the main cell wall components (Table 1). The maximum degradation rate of CDTA-soluble pectin (75.5%), Na_2CO_3 -soluble pectin (70.0%), hemicellulose (43.0%), and cellulose (44.8%) were reached at enzyme hydrolysis temperatures of 50, 45, 40, and 45 °C, respectively. The highest protein yield (78.54%) and the maximum yield of oil bodies (37.88%) was obtained at 55 °C and 50 °C, respectively, at which CDTA-soluble pectin had the best degradation rate. The degradation rates of CDTA-soluble pectin, Na_2CO_3 -soluble pectin, hemicellulose, and cellulose were 62.2% at 80 min enzyme hydrolysis time, 51.3% at 60 min, 55.3% at 60 min, and 62.6% at 100 min, respectively. The maximum protein yield (80%) and the maximum yield of oil bodies (37.92%) was recorded when CDTA-soluble pectin had the most optimal degradation rate and the enzyme hydrolysis time of 80 min (Fig. 1).

Table 1 Effects of Viscozyme® L on peanut cell wall compounds

Factors	CDTA soluble pectin (mg/100g)	Na_2CO_3 soluble pectin (mg/100g)	Hemicellulose (mg/100g)	Hemicellulose (mg/100g)	Cellulose (mg/100g)
Blank	18.02±1.19	12.89±1.19	74.39±3.09	468.12±24.02	468.12±24.02
1:2	8.97±0.45c	10.78±0.97a	58.13±7.89a	451.67±18.89a	451.67±18.89a
1:3	5.72±0.60d	3.25±0.37c	50.46±8.43a	200.60±13.78d	200.60±13.78d
1:4	5.88±0.57d	2.34±0.40d	47.46±7.90b	290.00±12.78c	290.00±12.78c
1:5	15.06±0.93b	2.38±0.36d	45.33±7.78b	446.67±22.11a	446.67±22.11a
1:6	16.97±1.00a	5.41±0.45b	45.42±7.76b	413.33±24.05b	413.33±24.05b
1:7	18.00±1.25a	5.38±0.49b	56.67±8.45a	456.67±20.06a	456.67±20.06a
0.25%	15.63±1.20a	10.66±1.00a	50.46±7.69a	456.33±11.45a	456.33±11.45a
0.50%	10.63±0.97b	7.76±0.67b	48.25±7.07a	401.67±8.05b	401.67±8.05b
0.75%	4.59±0.33f	5.09±0.35c	27.75±3.02d	397.60±7.89b	397.60±7.89b
1.00%	3.41±0.29g	4.08±0.07d	31.42±3.67c	210.00±7.46e	210.00±7.46e
1.25%	5.44±0.45e	3.09±0.11e	40.34±6.22b	223.00±8.56d	223.00±8.56d
1.50%	8.78±0.60d	3.34±0.23e	36.25±4.00b	373.33±9.45c	373.33±9.45c
1.75%	9.81±0.63c	5.69±0.45c	31.25±2.05c	398.33±10.09b	398.33±10.09b
2.00%	9.78±0.72c	7.13±0.45b	33.04±1.98c	371.67±8.98c	371.67±8.98c
35	16.47±0.95b	12.00±1.23a	68.79±9.19a	446.88±22.51a	446.88±22.51a
40	15.63±1.10b	4.31±0.99e	42.38±6.61c	354.62±16.88d	354.62±16.88d
45	7.13±0.80 c	3.91±0.65e	53.06±8.89b	258.33±13.56f	258.33±13.56f
50	4.41±0.62e	8.53±0.73b	58.75±8.77b	276.67±15.67e	276.67±15.67e
55	4.78±0.65e	6.34±0.80d	61.96±9.29a	376.01±17.76c	376.01±17.76c
60	5.56±0.77d	7.53±0.94c	64.71±9.07a	421.62±19.98b	421.62±19.98b
65	17.56±1.21a	10.67±1.03a	65.23±8.97a	438.55±18.33a	438.55±18.33a
70	17.87±1.08a	11.02±0.98a	67.79±9.08a	451.62±19.12a	451.62±19.12a
20min	14.94±1.08a	11.13±0.89a	69.92±9.82a	438.33±23.77a	438.33±23.77a
40min	12.56±0.96b	8.56±0.53b	70.55±9.94a	356.67±18.15c	356.67±18.15c
60min	11.84±0.99b	6.28±0.45d	33.25±1.53c	286.67±13.49d	286.67±13.49d
80min	6.81±0.65f	7.47±0.50c	43.96±5.79b	220.00±12.55e	220.00±12.55e
100min	6.91±0.59f	9.47±0.87b	46.00±5.93b	175.00±11.75f	175.00±11.75f
120min	8.69±0.76d	8.78±0.79b	48.29±6.22b	415.00±19.99b	415.00±19.99b
140min	7.44±0.80e	8.16±0.81b	47.00±6.03b	443.33±21.79a	443.33±21.79a
160min	9.59±0.77c	9.33±0.88b	46.71±5.90b	426.67±21.06a	426.67±21.06a

Note: different letters in each column indicate significant difference ($p < 0.05$) between each factor tested.

These data suggest a close correlation of the yield of protein and oil bodies with the degradation rates of

CDTA-soluble pectin, Na₂CO₃-soluble pectin, and cellulose. These results provide a theoretical basis for screening of optimum enzyme conditions for cell wall degradation.

3.3.

FT-IR spectra of cell wall polysaccharides

The characteristic spectra of pectin, hemicellulose, and cellulose exhibit a strong absorption band in the 1800-800 cm⁻¹ region (Yapo & Koffi, 2008). To reveal the effect of enzyme hydrolysis parameters on the main components in the cell wall of peanut, the characteristic wave numbers of cell wall polysaccharides under different extraction conditions were measured within two specific regions, 1800-1200 cm⁻¹ and 1200-800 cm⁻¹. FT-IR spectra are shown in Figs. 2-5, and the main characteristic wave numbers measured in the present study and infrared spectral wave numbers of cell wall polysaccharides in available literature are listed in Table 2.

Cellulose is a linear homopolymer composed of 1,4-linked β -D-Glcp units (1,4-linked β -D-glucan), while hemicellulose is a polymer composed of different types of monosaccharides such as pentose and hexose (e.g. xylose, arabinose, and galactose). Cellulose and hemicellulose are combined by hydrogen bond forming the network structure of cell wall which is filled with pectin (Frankova & Fry, 2013). In the case of plant cell wall, polysaccharides are bonded with each other, which may cause the slight shift of characteristic bands (Szymanska-Chargot & Zdunek, 2013). Slight differences were observed in the characteristic wave numbers of cell wall polysaccharides measured herein and those reported in previous studies (Kačuráková, Smith, & Gidley, 2002; Fellah, Anjukandi, & Waterland, 2009; Chatjigakis, 1998; Mccann, Defernez, & Urbanowicz, 2007; Synytsya, J Čopíková, & P Matějka, 2003) (Table 2).

Table 2 Absorption wave numbers obtained by FT-IR for assignment of cell wall polysaccharides

Frequency range (measured in this test) ^a	Frequency range (literature) ^b	Assignment ^c	Origin ^d	Comment
1739.7 (P)	1745-1740	C=O stretching vibration of alkyl ester	Pectin	CWM and CDTA
1610.5 (P)	1630-1600	COO ⁻ antisymmetric stretching	Polygalacturonic acid, carboxylate (pectin ester group)	Mainly CWM and CDTA residue
1361.7、1369.4、1361.713、1371.3 (XG, C)		CH ₂ bending	Xyloglucan, Cellulose	KOH residue All residue
1029.9 (C)				KOH residue
1313.5、1317.3 (C)	1317	CH ₂ symmetric bending	Cellulose	KOH residue
1230.5、1240.2、1265.312、1267.2 (P)		C–O stretching	Pectin	CWM and CDTA residue
1139.9 (XG)	1130	O–C–O asymmetric stretching	Xyloglucan (glycosidic link)	None
1035.7、1037.7 (XG)	1042	C–O stretching, C–C stretching	Xyloglucan (ring)	None
1029.9 (C)	1030	C–O stretching, C–C stretching	Cellulose (C6-H2-O6)	
1010.7、1014.5 (P)	1019	C–O stretching, C–C stretching	Pectin (C2-C3, C2-O2, C1-O1)	CWM and CDTA residue

997.2、1008.7 1010.7 (C)	1000	C-O stretching, C-C stretching	Cellulose (C6-H2-O6)	Na ₂ CO ₃ residue (potato)
----------------------------	------	-----------------------------------	-------------------------	---

Note: ^a the main wave numbers obtained in the present study; ^b the main wave numbers reported in the literature [30-34]; ^c functional groups; ^d molecules of the functional groups. CWM, cell wall material; CDTA, 2-cyclohexanediamine-*N,N,N',N'*-acetic acid; C, cellulose; P, pectin; XG, xyloglucan.

The effect of different extraction conditions (solid-liquid ratio, enzyme concentration, enzyme hydrolysis temperature, and enzyme hydrolysis time) on FT-IR spectra of celluloses are presented in Fig. 2. The main characteristic wave numbers of cellulose remained unchanged under different extraction conditions, but the absorbance, which denotes the content of characteristic wave numbers, varied significantly. Examples of FT-IR spectra of cellulose under different solid- liquid ratio are shown in Fig. 2a, cellulose had same characteristic wave numbers. However, characteristic bands of celluloses at solid- liquid ratio 1:3, 1:4, and 1:5 were sharper and more intensive compared to that at solid- liquid ratio 1:2. The solid- liquid ratio, enzyme concentration, enzyme hydrolysis temperature, and enzyme hydrolysis time exhibited a different degree of influence on the cellulose characteristic wave numbers, and changes of characteristic bands were corresponding to the acting sites of Viscozyme[®] L on cellulose. Similar results were observed for hemicellulose, CDTA-soluble pectin, and Na₂CO₃-soluble pectin (Figs.3-5).

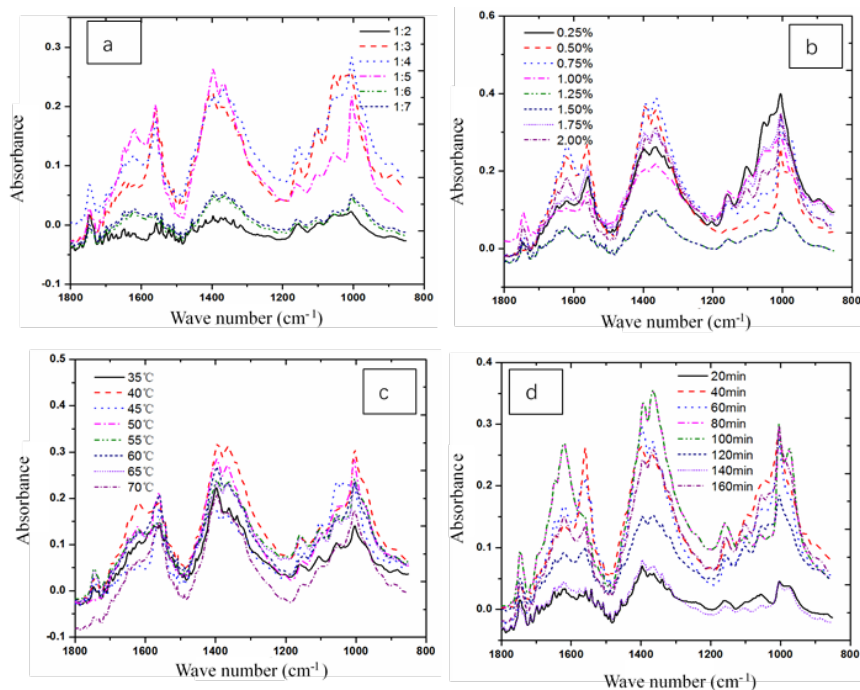


Fig. 2 FT-IR spectra of cellulose under different extraction conditions.

(a: solid- liquid ratio; b: enzyme concentration; c: enzyme hydrolysis temperature; d: enzyme hydrolysis time)

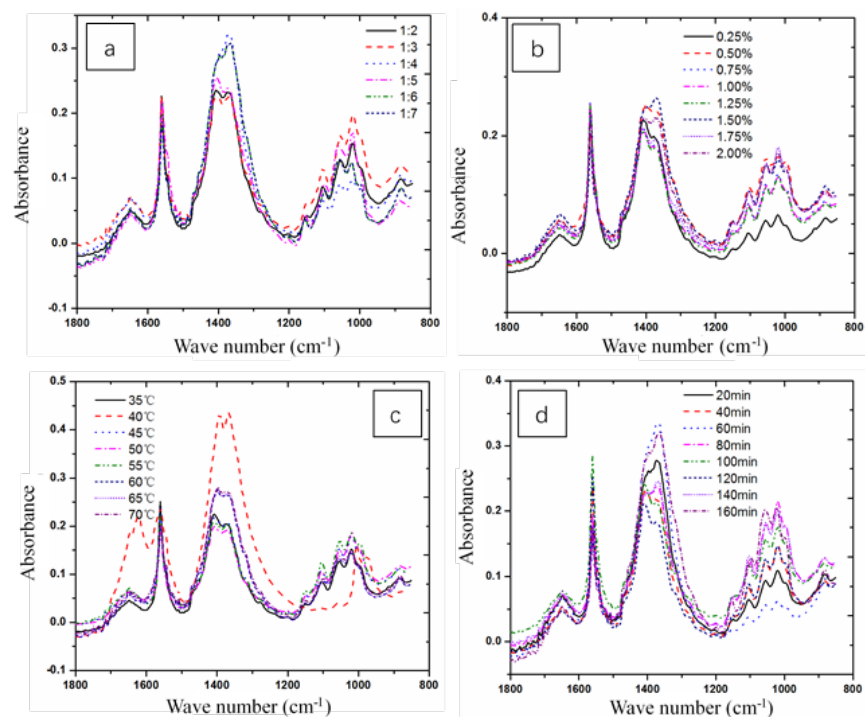


Fig. 3 FT-IR spectra of hemicellulose under different extraction conditions.

(a: solid-liquid ratio; b: enzyme concentration; c: enzyme hydrolysis temperature; d: enzyme hydrolysis time)

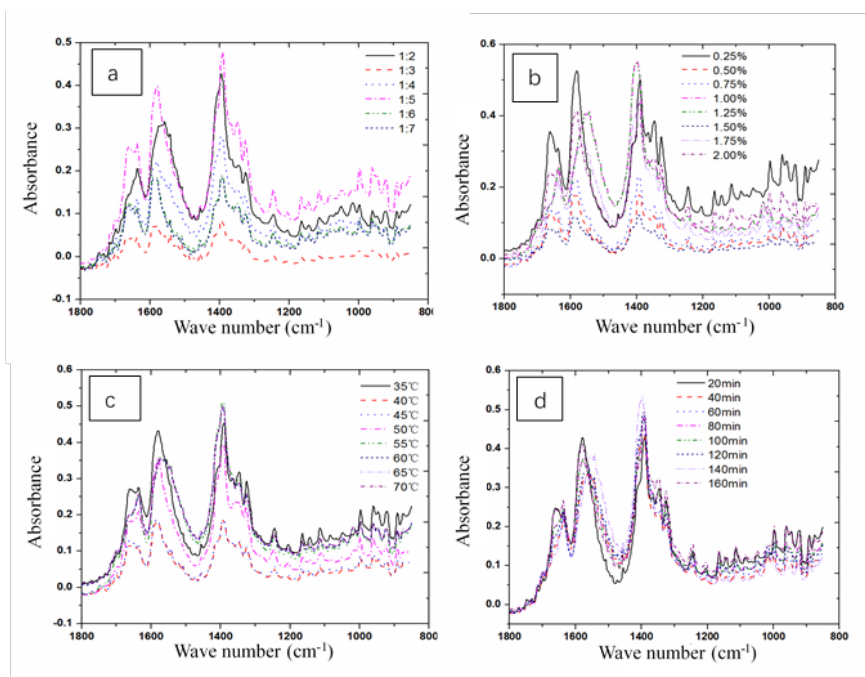


Fig. 4 FT-IR spectra of CDTA soluble pectin under different extraction conditions.

(a: solid-liquid ratio; b: enzyme concentration; c: enzyme hydrolysis temperature; d: enzyme hydrolysis time)

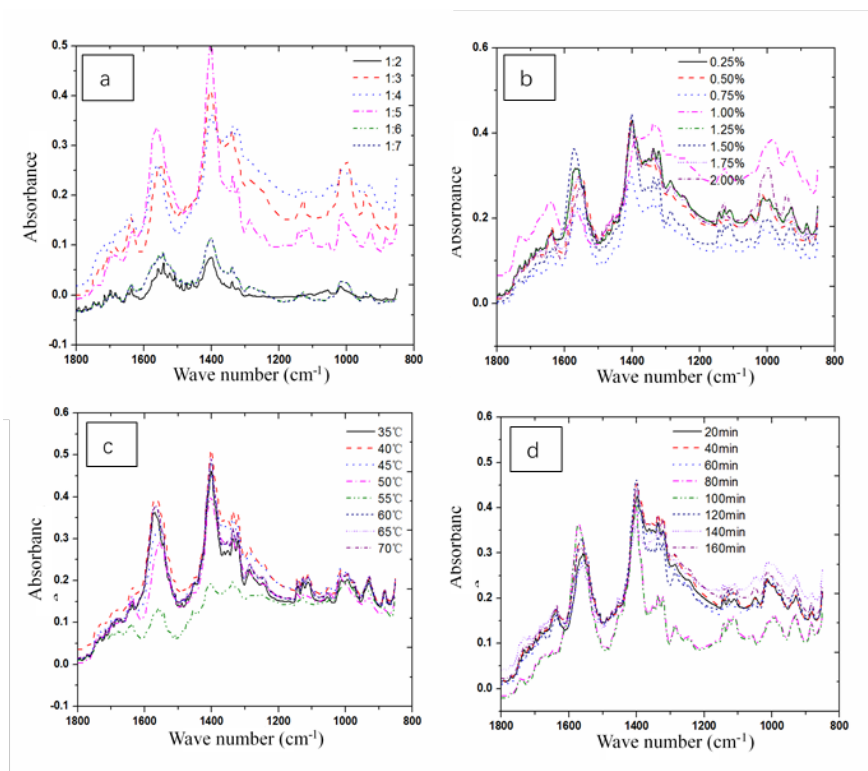


Fig. 5 FT-IR spectra of Na_2CO_3 -soluble pectin under different extraction conditions.

(a: solid-liquid ratio; b: enzyme concentration; c: enzyme hydrolysis temperature; d: enzyme hydrolysis time)

3.4. PCA of characteristic wave numbers of cell wall polysaccharides

The PCA scatter plots of the FT-IR spectra of cell wall polysaccharides in the 1800-800 cm^{-1} region is shown in Fig. 6. The changes of infrared spectroscopy in the main components of the cell wall (cellulose, hemicellulose, and pectin) under different extraction conditions were explained by PC1 and PC2. PC1 and PC2 indicated that cell wall residues were grouped or scattered in group along the PC2 axis and PC1 axis, respectively. Not only reflected difference between groups of cellulose, hemicellulose, and pectin, but also reflected differences in the group of cellulose, hemicellulose, and pectin affected by solid-liquid ratio, enzyme concentration, enzyme hydrolysis temperature, and enzyme hydrolysis time.

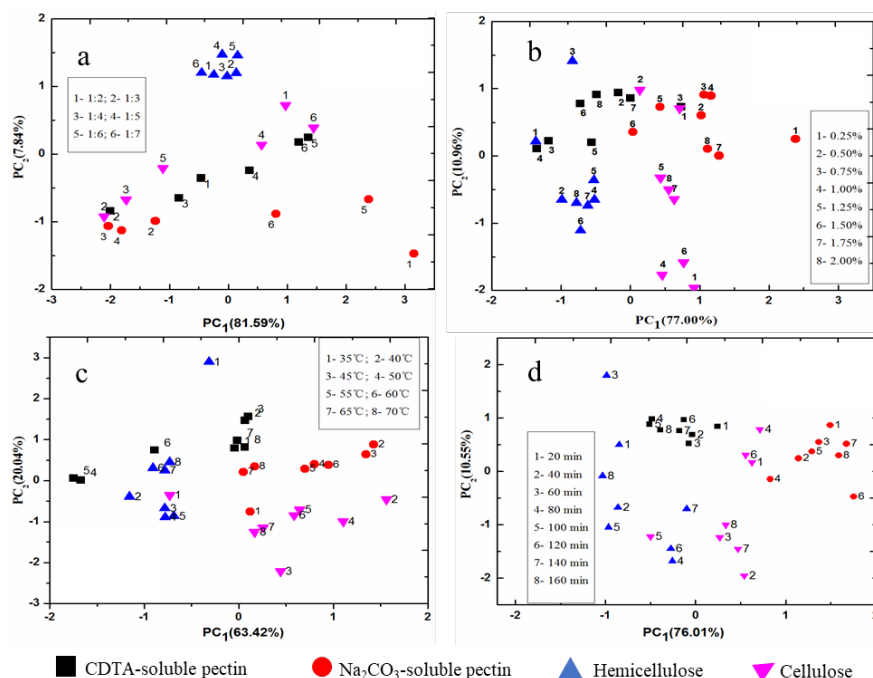


Fig. 6 PCA score scatter plots of peanut cell wall FT-IR spectra in the 1800-800 cm^{-1} region for pectin, hemicellulose, and cellulose under different extraction conditions.

(a: solid-liquid ratio; b: enzyme concentration; c: enzyme hydrolysis temperature; d: enzyme hydrolysis time)

The scores scatter plots PC1 (explained 81.59% of variability) and PC2 (explained 7.84% of variability) were used to obtain separation of each group of cell wall polysaccharides in 1800-800 cm^{-1} region at different solid-liquid ratios (Fig. 6a). The scores scatter plot PC1 vs. PC2 indicates that the cell wall polysaccharides are grouped along the PC2 axis and scattered along the PC1 axis. The tendency for the location of scores of cell wall polysaccharides was going from positive to negative values along the PC1 axis, indicating that the solid-liquid ratio exerted a strong effect on characteristic wave numbers of CDTA-soluble pectin, Na_2CO_3 -soluble pectin, cellulose, and hemicellulose. The high coefficients of infrared wave values in the component matrix (Table 3) indicated that the corresponding group played a larger role in the enzymatic hydrolysis of the cell wall. The characteristic wave numbers of cellulose influenced by liquid-solid ratio were 997.2, 1008.7, 1010.7, 1313.5, and 1317.3 cm^{-1} and they were related to the C-O stretching, C-C stretching, and the CH_2 symmetrical bending of cellulose. The characteristic wave numbers of hemicellulose were 960.5, 1037.7, and 1139.9 cm^{-1} , and they were assigned to the C-O stretching, C-C stretching, and O-C-O asymmetrical bending of hemicellulose. Furthermore, the characteristic wave numbers of pectin were 1010.7, 1014.5, 1265.3, and 1267.2 cm^{-1} , and they acted on the C-O stretching and C-C stretching of pectin.

The scores scatter plot shown in Figs. 6b-d allow the distinction of each group of cell wall polysaccharides in 1800-800 cm^{-1} region at different enzyme concentrations, enzyme hydrolysis temperatures, and enzyme hydrolysis times along the PC1 axis, which corresponds to 77.00, 63.42, and 76.01% of the variability contained in the FT-IR spectra, respectively. The scores scatter plot PC1 vs. PC2 indicates that the cell wall polysaccharides are grouped along the PC2 axis and scattered along the PC1 axis. The scores of cellulose and Na_2CO_3 -soluble pectin lay on the positive side of PC1 scores, while CDTA-soluble pectin and hemicellulose were on the negative side of PC1. Clear grouping of cell wall polysaccharides was obtained under different enzyme concentrations, enzyme hydrolysis temperatures, and enzyme hydrolysis times, indicating that enzymatic conditions had strong effect on cell wall polysaccharides. The characteristic wave numbers

of cellulose influenced by enzyme concentration were 997.2, 1010.7, 1313.5, 1317.3 cm^{-1} , and they acted on the C-O stretching, C-C stretching, and CH_2 symmetrical bending of cellulose; the characteristic wave numbers of hemicellulose were 960.5 and 1139.9 cm^{-1} , and they acted on the O-C-O asymmetrical bending of hemicellulose; the characteristic wave numbers of pectin were 1010.7, 1230.5, 1265.3, and 1267.2 cm^{-1} , and they acted on the C-O stretching and C-C stretching of pectin (Fig.6b and Table 3). The characteristic wave numbers of cellulose influenced by enzyme hydrolysis temperature were 997.2, 1008.7, and 1010.7 cm^{-1} ; they acted on the C-O stretching and C-C stretching of cellulose; the characteristic wave numbers of hemicellulose were 960.5, 1037.7, and 1139.9 cm^{-1} , and they acted on the C-O stretching, C-C stretching, and O-C-O asymmetrical bending of hemicellulose; the characteristic wave numbers of pectin were 1010.7, 1230.5, 1265.3, and 1267.2 cm^{-1} , and they acted on the C-O stretching and C-C stretching of pectin (Fig.6b and Table 3). As shown in Fig. 6d and Table 3, the characteristic wave numbers of cellulose influenced by enzymatic time were 997.2, 1010.7, 1313.5, and 1317.3 cm^{-1} , which acted on the C-O stretching, C-C stretching, and CH_2 symmetrical bending of cellulose; the characteristic wave number of hemicellulose was 1139.9 cm^{-1} , which acted on the O-C-O asymmetrical bending of hemicellulose; the characteristic wave numbers of pectin were 1010.7, 1014.5, 1230.5, 1265.3, and 1267.2 cm^{-1} , which acted on the C-O stretching and C-C stretching of pectin.

Table 3 Component matrix of principal component analysis

Wave length	Wave length	Solid-liquid ratio/ g / mL	Solid-liquid ratio/ g / mL	Solid-liquid ratio/ g / mL	Solid-liquid ratio/ g / mL	Solid-liquid ratio/ g / mL	Solid-liquid ratio/ g / mL	enzymatic concentration/ %	enzymatic concentration/ %	enzymatic concentration/ %	enzyme hydrolysis temperature / $^{\circ}\text{C}$	enzyme hydrolysis temperature / $^{\circ}\text{C}$	enzyme hydrolysis temperature / $^{\circ}\text{C}$	enzyme hydrolysis temperature / $^{\circ}\text{C}$	enzyme hydrolysis temperature / $^{\circ}\text{C}$
Cellulose	997.159	PC ₁	PC ₁	PC ₁	PC ₂	PC ₁	PC ₁	PC ₁	PC ₁	PC ₂	PC ₂	PC ₂	PC ₁	PC ₁	PC ₁
	1008.732	0.997	0.928	-	-	-	0.945	0.945	-	-	-	0.961	0.961	0.036	0.036
	1010.660	0.911	0.895	0.292	0.292	0.292	0.179	0.179	0.179	0.179	0.179	0.936	0.936	0.109	0.109
	1029.948	0.844	0.844	0.381	0.381	0.381	0.311	0.311	0.311	0.311	0.311	0.946	0.946	0.123	0.123
	1313.473	0.965	0.965	0.386	0.386	0.386	0.326	0.326	0.326	0.326	0.326	0.897	0.897	0.319	0.319
	1317.330	0.952	0.952	0.517	0.517	0.517	0.591	0.591	0.591	0.591	0.591	0.973	0.973	-	-
	1361.691	0.838	0.838	0.235	0.235	0.235	0.832	0.832	0.498	0.498	0.498	0.965	0.965	0.076	0.076
	1369.406	0.809	0.809	0.273	0.273	0.273	0.805	0.805	0.521	0.521	0.521	0.858	0.858	0.102	0.102
	1371.335	0.812	0.812	0.302	0.302	0.302	0.641	0.641	0.696	0.696	0.696	0.843	0.843	0.329	0.329
	1371.335	0.812	0.812	0.305	0.305	0.305	0.602	0.602	0.704	0.704	0.704	0.843	0.843	0.351	0.351
Hemicellulose	960.513	0.913	0.913	0.032	0.032	0.032	0.740	0.740	0.257	0.257	0.257	0.913	0.913	-	-
	1035.734	0.852	0.852	-	-	-	0.723	0.723	-	-	-	0.899	0.899	0.292	0.292
	1037.663	0.858	0.858	0.509	0.509	0.509	0.596	0.596	0.596	0.596	0.596	0.905	0.905	0.279	0.279
	1139.886	0.915	0.915	0.496	0.496	0.496	0.583	0.583	0.583	0.583	0.583	0.936	0.936	-	-
	1361.691	0.838	0.838	0.145	0.145	0.145	0.719	0.719	0.206	0.206	0.206	0.858	0.858	0.323	0.323
	1371.335	0.812	0.812	0.310	0.310	0.310	0.608	0.608	0.701	0.701	0.701	0.844	0.844	0.346	0.346

Wave length	Wave length										enzyme	enzyme	enzyme	enzyme	enzyme
		Solid-liquid ratio/g / mL	Solid-liquid ratio/g / mL	Solid-liquid ratio/g / mL	Solid-liquid ratio/g / mL	Solid-liquid ratio/g / mL	Solid-liquid ratio/g / mL	enzymatic content/%	enzymatic content/%	enzymatic content/%	tem-perature /°C	tem-perature /°C	tem-perature /°C	tem-perature /°C	tem-perature /°C
Pectin	1010.660	1010.660	0.911	-	-	-	0.923	0.923	-	-	-	0.946	0.946	0.123	0.123
				0.386	0.386	0.386			0.280	0.280	0.280				
	1014.518	1014.518	0.908	-	-	-	0.873	0.873	-	-	-	0.946	0.946	0.165	0.165
				0.397	0.397	0.397			0.421	0.421	0.421				
	1230.537	1230.537	0.884	0.287	0.287	0.287	0.903	0.903	-	-	-	0.897	0.897	-	-
									0.204	0.204	0.204			0.409	0.409
	1240.181	1240.181	0.876	0.313	0.313	0.313	0.894	0.894	-	-	-	0.889	0.889	-	-
									0.041	0.041	0.041			0.421	0.421
	1265.254	1265.254	0.915	0.249	0.249	0.249	0.928	0.928	0.123	0.123	0.123	0.926	0.926	-	-
														0.315	0.315
	1267.183	1267.183	0.917	0.243	0.243	0.243	0.932	0.932	0.098	0.098	0.098	0.928	0.928	-	-
														0.304	0.304
	1610.499	1610.499	0.691	0.329	0.329	0.329	0.719	0.719	0.063	0.063	0.063	0.766	0.766	-	-
														0.241	0.241
	1739.725	1739.725	0.826	0.137	0.137	0.137	0.628	0.628	-	-	-	0.805	0.805	-	-
									0.470	0.470	0.470			0.433	0.433

The above results indicate that Viscozyme® L acted on the C-O stretching, C-C stretching, and CH₂ symmetrical bending of cellulose, the C-O stretching and O-C-O asymmetrical bending of hemicellulose, and the C-O stretching and C-C stretching of pectin during the process of aqueous enzymatic extraction (Fig. 7).

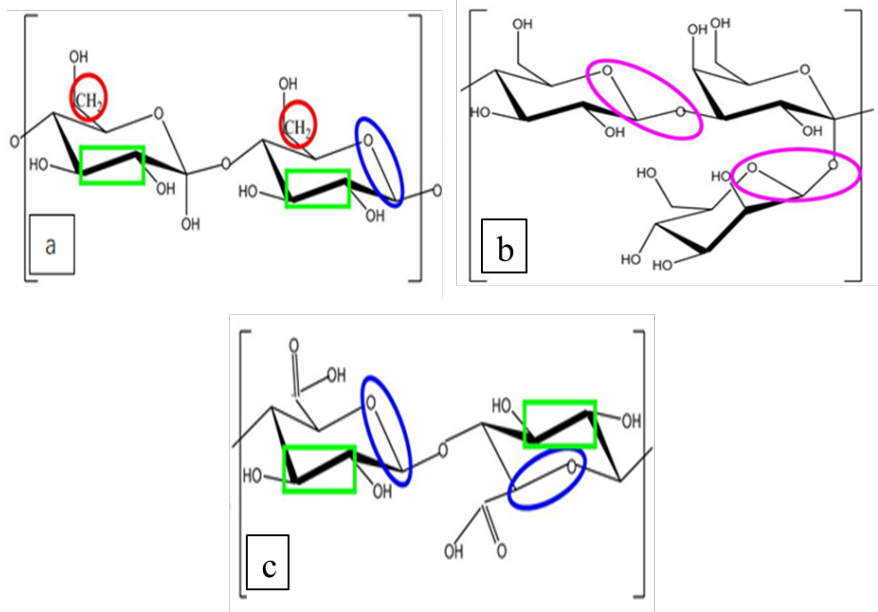


Fig. 7 Molecular structure of cellulose (a), pectin (b), and hemicellulose (c).

3.5. The mechanism of aqueous enzymatic extraction of protein and oil bodies

The mechanism of the protein and oil body extraction through the enzymatic hydrolysis of the peanut cell wall is presented schematically in Fig. 8. Proteins and oils are present in peanut cotyledon cells in the form of protein bodies and oil bodies. The cell wall, which is composed of cellulose, hemicellulose, and pectin, maintains the cell structure and inhibits the release of proteins and oils. In the aqueous enzymatic extraction process, mechanical crushing is an important step that destroys the peanut cell wall and promotes the release of proteins and oil bodies. We used the conventional dry crushing in this study to break the chain structure of the cell wall and decrease the peanut particle size. However, dry crushing destroyed only a part of peanut cells, and therefore not all protein and oil bodies were released. In contrast, Viscozyme[®] L degraded sufficiently the structure of the cell wall by acting on the C-O stretching, C-C stretching, and CH₂ symmetrical bending of cellulose, the C-O stretching and O-C-O asymmetrical bending of hemicellulose, and the C-O stretching and C-C stretching of pectin, and thus facilitated the release of oil bodies and proteins from peanut cells. After centrifugation of the extract, which contained proteins, oil bodies, and the enzymatic hydrolysate of cell wall polysaccharides, oil bodies exist in the upper layer of the aqueous phase, while proteins and enzymatic hydrolysate are in the aqueous phase.

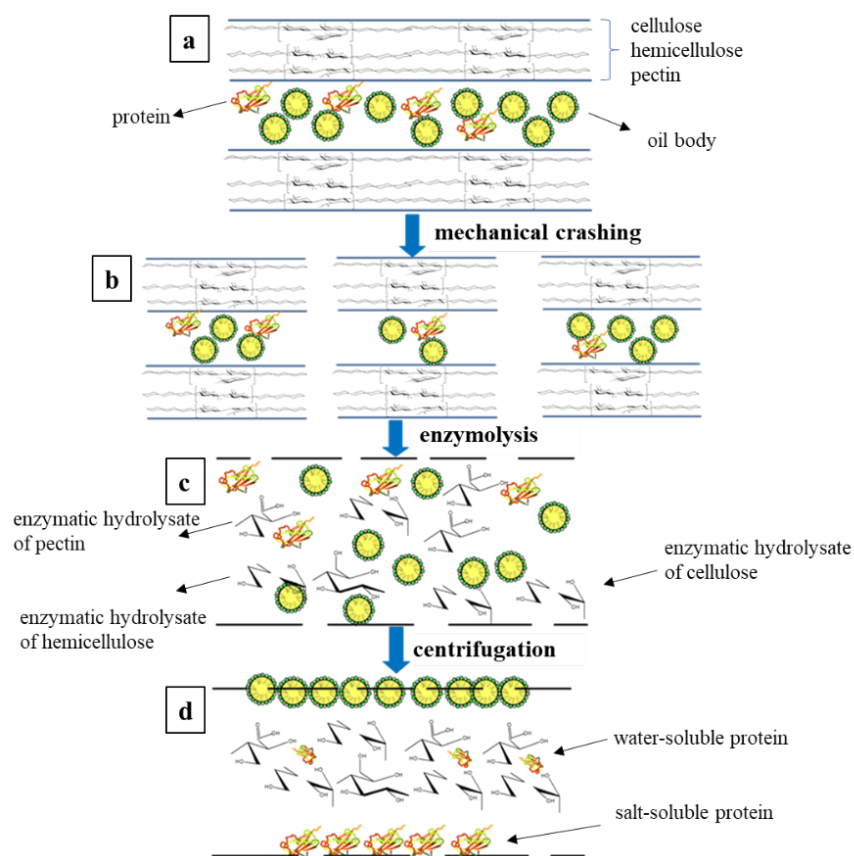


Fig. 8 Schematic diagram of the mechanism of enzymatic extraction of proteins and oil bodies from peanut seeds.

4. Conclusions

The extraction of oil bodies and peanut protein was closely related to the degree to which the main compo-

nents of the peanut cell wall were degraded. The yield of peanut protein and oil bodies was positively correlated to the degradation rate of CDTA-soluble pectin, Na₂CO₃-soluble pectin, and cellulose. Viscozyme[®] L degraded the cellulose, hemicellulose, and pectin molecules and destroyed the structure of the cell wall to a greater extent compared with mechanical degradation. Viscozyme[®] L acted on the C-O stretching, C-C stretching, and CH₂ symmetrical bending of cellulose, the C-O stretching and O-C-O asymmetrical bending of hemicellulose, and the C-O stretching and C-C stretching of pectin. This, in turn, facilitated the release of oil bodies and proteins from the cells. The mechanism of cell wall degradation was preliminarily discussed by analyzing the changes in the structure of cell wall polysaccharides and the key sites of Viscozyme[®] L action on peanut cell wall during enzymatic hydrolysis. These data will provide theoretical basis for further research on the mechanism of aqueous enzymatic extraction.

Acknowledgements

This study was supported by the National Natural Science Foundation of China (21676073).

Author Contributions

C. Liu and L. Hao designed and conducted the experiments, performed data analysis, and wrote the manuscript. F. Chen supervised the study and helped to initiate the project. T. Zhu revised the manuscript.

Conflict of Interest

We declare that we have no conflict of interest.

References

- Ana Alonso-Simón, Encina A E, & Penélope García-Angulo. (2004). FTIR spectroscopy monitoring of cell wall modifications during the habituation of bean (*Phaseolus vulgaris* L.) callus cultures to dichlobenil. *Plant Science (Oxford)* . 167(6), 1280-1281. <https://doi.org/10.1016/j.plantsci.2004.06.025>
- Balvardi M, Rezaei K, & Mendiola J A. (2015). Optimization of the Aqueous Enzymatic Extraction of Oil from Iranian Wild Almond. *Journal of the American Oil Chemists' Society* . 92(7), 985-992. <https://doi.org/10.1007/s11746-015-2671-y>
- Barros A S, Mafra I, & Ferreira D. (2002). Determination of the degree of methylesterification of pectic polysaccharides by FT-IR using an outer product PLS1 regression. *Carbohydrate Polymers* . 50(1), 85-94. [https://doi.org/10.1016/S0144-8617\(02\)00017-6](https://doi.org/10.1016/S0144-8617(02)00017-6)
- Bisht T S, Sharma S K, & Sati R C. (2015). Improvement of efficiency of oil extraction from wild apricot kernels by using enzymes. *Journal of Food Science and Technology* . 52(3), 1543-1551. <https://doi.org/10.1007/s13197-013-1155-z>
- Campbell, K. A., Glatz, & C. E. (2011). Advances in aqueous extraction processing of soybeans. *Journal of American Oil Chemist's Society* . 88(4), 449-465. <https://doi.org/10.1007/s11746-010-1724-5>
- Chatjigakis A K. (1998). FT-IR spectroscopic determination of the degree of esterification of cell wall pectins from stored peaches and correlation to textural changes. *Carbohydr. Polym.* 37(4), 395-408. [https://doi.org/10.1016/S0144-8617\(98\)00057-5](https://doi.org/10.1016/S0144-8617(98)00057-5)
- Coimbra M A, Barros A, & Barros M. (1998). Multivariate analysis of uronic acid and neutral sugars in whole pectic samples by FT-IR spectroscopy. *Carbohydrate Polymers*. 37(3), 241-248. [https://doi.org/10.1016/S0144-8617\(98\)00066-6](https://doi.org/10.1016/S0144-8617(98)00066-6)
- Fellah A, Anjukandi P, & Waterland M R. (2009). Determining the degree of methylesterification of pectin by ATR/FT-IR: Methodology optimisation and comparison with theoretical calculations. *Carbohydrate Polymers* . 78(4), 847-853. <https://doi.org/10.1016/j.carbpol.2009.07.003>
- Ferreira D, Barros A, & Coimbra M A. (2001). Use of FT-IR spectroscopy to follow the effect of processing in cell wall polysaccharide extracts of a sun-dried pear. *Carbohydrate Polymers*. 45(2), 175-182.

[https://doi.org/10.1016/S0144-8617\(00\)00320-9](https://doi.org/10.1016/S0144-8617(00)00320-9)

Frankova L & Fry S C. (2013). Biochemistry and physiological roles of enzymes that ‘cut and paste’ plant cell-wall polysaccharides. *Journal of Experimental Botany* , 64(12):3519-3550. <https://doi.org/10.1093/jxb/ert01>

Fry S C & Fry S. (1988). The Growing Plant Cell Wall: Chemical and Metabolic Analysis. *Growing Plant Cell Wall Chemical & Metabolic Analysis* , 27(12), 4008.

Gao J F. (2006). Experimental guidance on plant physiology. Higher Education Press. Beijing, China. pp. 140-150.

Gaur R, Sharma A, & Khare S K. (2007). A novel process for extraction of edible oils: Enzyme assisted three phase partitioning (EATPP). *Bioresource Technology* , 98(3): 696-699. <https://doi.org/10.1016/j.biortech.2006.01.023>

Gnanasambandam R & Proctor A. (2000). Determination of pectin degree of esterification by diffuse reflectance Fourier transform infrared spectroscopy. *Food Chemistry* . 68(3), 327-332. [https://doi.org/10.1016/S0308-8146\(99\)00191-0](https://doi.org/10.1016/S0308-8146(99)00191-0)

Han Y S. (1992). Food chemistry experiment guide. Beijing agricultural university press. Beijing, China. pp. 19-21.

He C W. (2015). Chemical evidence and functional study of silicon - hemicellulose complex in cell wall of rice (*Oryza sativa*). Huazhong Agricultural University. Wuhan, China. <https://doi.org/10.7666/d.Y2803337>

He X Q. (2015). Multivariate statistical analysis, 4th Ed. China Renmin University Press. Beijing, China. pp. 114-128.

Hou M L. (2004). Food analysis. Chemical Industry Press. Beijing, China. vol. 5, pp. 89-90.

Hori R & Sugiyama J. (2003). A combined FT-IR microscopy and principal component analysis on softwood cell walls. *Carbohydrate Polymers* . 52(4), 449-453. [https://doi.org/10.1016/S0144-8617\(03\)00013-4](https://doi.org/10.1016/S0144-8617(03)00013-4)

Kačuráková M, Smith A C, & Gidley M J. (2002). Molecular interactions in bacterial cellulose composites studied by 1D FT-IR and dynamic 2D FT-IR spectroscopy. *Carbohydrate Research* . 337(12), 1145-1153. [https://doi.org/10.1016/S0008-6215\(02\)00102-7](https://doi.org/10.1016/S0008-6215(02)00102-7)

Latif S, Anwar F, & Hussain A I. (2011). Aqueous enzymatic process for oil and protein extraction from *Moringa oleifera* seed. *European Journal of Lipid Science & Technology* . 113(8), 1012-1018. <https://doi.org/10.1002/ejlt.20100052>

Li H, Han T, & Jin P. (2014). Study on degradation characteristics of cell wall polysaccharides during post-ripening and softening of winter jujube. *Journal of Chinese Institute of Food Science and Technology* . 14(2), 109-117. <https://doi.org/10.16429/j.1009-7848.2014.02.016>

Li T, Peng Y, & Li Q. (2015). Study on extraction and structure of four kinds of peanut proteins. *Journal of Food Science and Technology*. 33(3), 35-42. <https://doi.org/10.3969/j.issn.2095-6002.2015.03.007>

Li Y, Qi B K, & Sui X N. (2016). Study on high pressure steam demulsification of peanut oil extracted by enzyme-assisted aqueous extraction. *China Oils and Fats* . 41(7), 6-9. <https://doi.org/10.3969/j.issn.1003-7969.2016.07.002>

Liu J J, Gasmalla M A A, & Li P. (2016). Enzyme-assisted extraction processing from oilseeds: Principle, processing and application. *Innovative Food Science & Emerging Technologies* . 35, 184-193. <https://doi.org/10.1016/j.ifset.2016.05.002>

LIU Yan, ZHAO Guan-li, & SU Xin-guo. (2013). Functional and Conformational Properties of Arachin and Conarachin. *Modern Food Science and Technology* . 29(9), 2095-2101. <https://doi.org/CNKI:SUN:GZSP.0.2013-09-011>

Mat Yusoff, M., Gordon, M.H., & Niranjana, K. (2015). Aqueous enzyme assisted oil extraction from oilseeds and emulsion de-emulsifying methods: a review. *Trends Food Sci. Technol* . 41 (1), 60-82. <https://doi.org/10.1016/j.tifs.2014.09.009>

Mccann M C, Defernez M, & Urbanowicz B R. (2007). Neural Network Analyses of Infrared Spectra for Classifying Cell Wall Architectures. *Plant Physiology* . 143(3), 1314-1326. <https://doi.org/10.1104/pp.106.093054>

Sukhotu R. (2014). Aqueous enzymatic extraction method of Maize Germ oil bodies and their physiochemical properties. China Agricultural University. Beijing, China.

Synytsya A, J Čopíková, & P Matějka. (2003). Fourier transform Raman and infrared spectroscopy of pectins. *Carbohydrate Polymers* . 54(1), 97-106. [https://doi.org/10.1016/S0144-8617\(03\)00158-9](https://doi.org/10.1016/S0144-8617(03)00158-9)

Szymanska-Chargot M & Zdunek A. (2013). Use of FT-IR spectra and PCA to the bulk characterization of cell wall residues of fruits and vegetables along a fraction process. *Food biophysics* . 8(1), 29-42. <https://doi.org/10.1007/s11483-012-9279-7>

Szydłowska-Czerniak A, Karlovits G, & Hellner G. (2010). Effect of enzymatic and hydrothermal treatments of rapeseeds on quality of the pressed rapeseed oils: part II. Oil yield and oxidative stability. *Process Biochemistry* , 45(2): 247-258. <https://doi.org/10.1016/j.procbio.2009.09.014>

Winning H, Viereck N, & Salomonsen T. (2009). Quantification of blockiness in pectins-A comparative study using vibrational spectroscopy and chemometrics. *Carbohydr Res* . 344(14), 1833-1841. <https://doi.org/10.1016/j.carres.2008.11.014>

XU Fei, LIU Li, & SHI Aimin. (2016). Composition, structures and functional properties of peanut seed protein at subunit level: a review. *Food Science* . 37(7), 264-269. <https://doi.org/10.7506/spkx1002-6630-201607047>

Yapo B M & Koffi K L. (2008). The polysaccharide composition of yellow passion fruit rind cell wall: chemical and macromolecular features of extracted pectins and hemicellulosic polysaccharides. *Journal of the Science of Food and Agriculture* , 88(12):2125-2133. <https://doi.org/10.1002/jsfa.3323>

Zúñiga M E, Soto C, & Mora A. (2003). Enzymic pre-treatment of Guevina avellana mol oil extraction by pressing. *Process Biochemistry* , 39(1): 51-57. [https://doi.org/10.1016/s0032-9592\(02\)00286-8](https://doi.org/10.1016/s0032-9592(02)00286-8)

Hosted file

Figures.docx available at <https://authorea.com/users/307433/articles/444263-the-mechanism-of-extraction-of-peanut-protein-and-oil-bodies-by-enzymatic-hydrolysis-of-the-cell-wall>

Hosted file

Tables.docx available at <https://authorea.com/users/307433/articles/444263-the-mechanism-of-extraction-of-peanut-protein-and-oil-bodies-by-enzymatic-hydrolysis-of-the-cell-wall>